4.1 Some Comments on Fuselage Drag

Jan Roskam
University of Kansas

Introduction

This paper focuses on the following areas relating to fuselage drag:

1. Fuselage fineness - ratio and why and how this can be selected during preliminary design;
2. Windshield drag;
3. Skin roughness; and
4. Research needs in the area of fuselage drag.

Fuselage Fineness Ratio and How It Can Be Selected

Table 1 presents some data on fuselage fineness ratios for several current general aviation airplanes. It is interesting to note, that with one exception, all have values of around $\ell_B/d = 5$ to 6. In Reference 1, the fuselage (or body) drag is estimated from:

$$C_{D_{o_B}} = C_{f_B}\left[1 + \frac{60}{(\ell_B/d)^3} + .0025\left(\frac{\ell_B}{d}\right)\right]\frac{S_{wet_{body}}}{S_{wing}} \qquad (1)$$

This equation assumes zero base drag. Figure 1 shows how the [ ]-term in equation (1) is related to ℓ_B/d. Note that the [ ]-term no longer decreases significantly significantly after $\ell_B/d = 6.0$ is exceeded. This would indeed suggest that values of 5 to 6 for ℓ_B/d are about optimum. However, there are three other factors to contend with:

1. increasing ℓ_B/d will decrease C_{f_B};
2. increasing ℓ_B/d will increase $S_{wet_{body}}$; and
3. increasing ℓ_B/d will decrease tail wetted area requirements, for constant stability levels.

It appears that a more detailed examination of fuselage fineness ratio is therefore in order. The next section presents a method for minimizing the sum of fuselage and empennage friction drag, under a constant directional and longitudinal stability constraint.

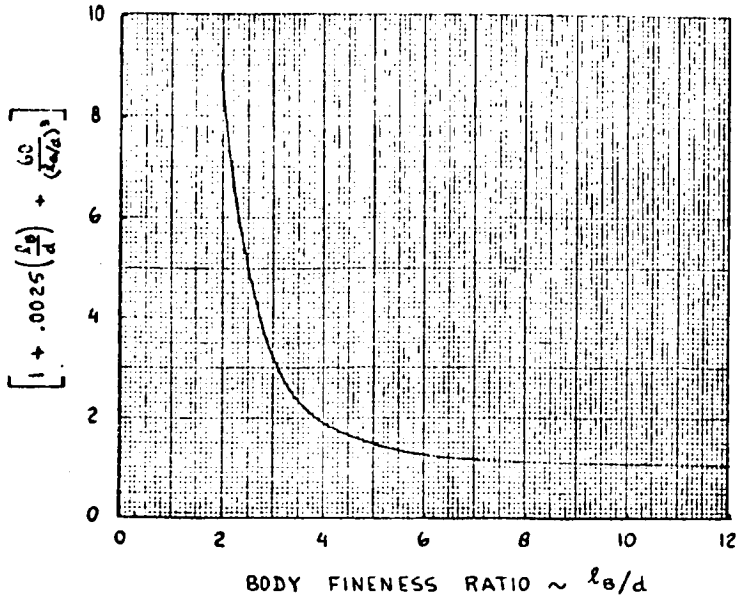

Figure 1. Body Zero-Lift Drag Factor as a Function of Body Fineness Ratio

Table 1. Examples of Fuselage Fineness Ratios and Wetted Areas for General Aviation Aircraft

Type	$\frac{\ell_B}{d}$	S_{wing}	$S_{wet\ body}$	$\frac{S_{wet\ body}}{S_{wing}}$
Cessna 210	5.02	175	319	1.82
Cessna 207	5.69	174	425	2.44
Beech Sierra	5.22	146	332	2.27
Cessna 185	5.15	176	292	1.68
Beech Bonanza ('58)	4.98	181	323	1.78
Beech Baron	5.69	199.2	362	1.82
Piper Navajo	5.97	229	502	2.19
Cessna 310	5.40	179	306	1.71
Piper Seneca	5.68	206.5	356	1.72
Beech Duke	5.59	212.9	586	2.28
Cessna 414	5.52	195.7	488	2.49
Beech King Air	6.06	294	652	2.22
Gates Learjet 24	8.8	232	502	2.16

A Method for Minimizing General Aviation Airplane Fuselage and Empennage Friction Drag

Fuselage Drag - The objective is to show how fuselage drag and empennage friction drag can be estimated under constant static stability constraints.

It is assumed that the fuselage from nose to passenger compartment is defined roughly as in Figure 2.

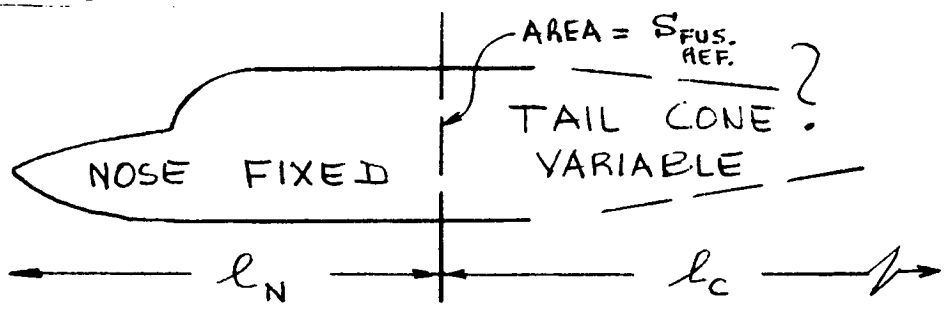

Figure 2. Definition of Fuselage in Two Parts

It is also assumed that the tail cone can be represented by a skewed cone as in Figure 3.

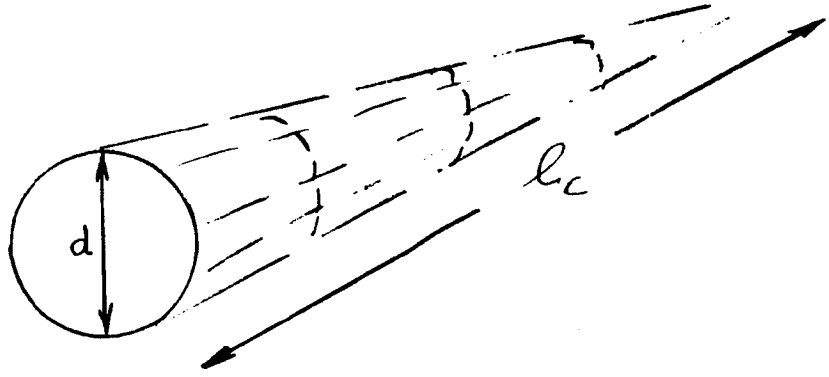

Figure 3. Modeling Aft Fuselage as a Skewed Cone

The equivalent fuselage diameter is defined such that:

$$\frac{\pi}{4} d^2 = S_{\substack{FUS. \\ REF.}} \Rightarrow d = \sqrt{\frac{4 S_{FUS\ REF}}{\pi}} \qquad (2)$$

The wetted area of the fuselage can now be written as:

$$S_{\substack{WET \\ BODY}} = S_{\substack{WET \\ NOSE}} + S_{\substack{WET \\ CONE}} = S_{\substack{WET \\ NOSE}} + F \cdot \pi \cdot \frac{d}{2} \sqrt{\left(\frac{d}{2}\right)^2 + \ell_C^2} \qquad (3)$$

where F is a correction factor accounting for the fact that the rear fuselage is not a cone. F can be found by comparison to existing aircraft.

The Fuselage Drag coefficient (zero-lift) can be expressed as:

$$C_{D_{o_{FUS.}}} = C_{F_B}\left[1 + \frac{60}{\{(\ell_N+\ell_c)/d\}^3} + .0025\left(\frac{\ell_N+\ell_c}{d}\right)\right]\frac{S_{WET_{BODY}}}{S_{wing}} R_{WB} \quad (4)$$

All symbols are defined in Reference 1. Fuselage base drag is neglected. For given ℓ_c, $C_{D_{of_{us}}}$ can thus be computed as a function of ℓ_c.

Empennage Drag - The horizontal tail wetted area may be approximated by:

$$S_{WET_{H.T.}} = S_H\left(2 + \underset{<<1.0}{f(t/c)}\right) - C_{R_H}^2 \frac{d}{\ell_c} \quad (5)$$

where the geometry is defined in Figure 4.

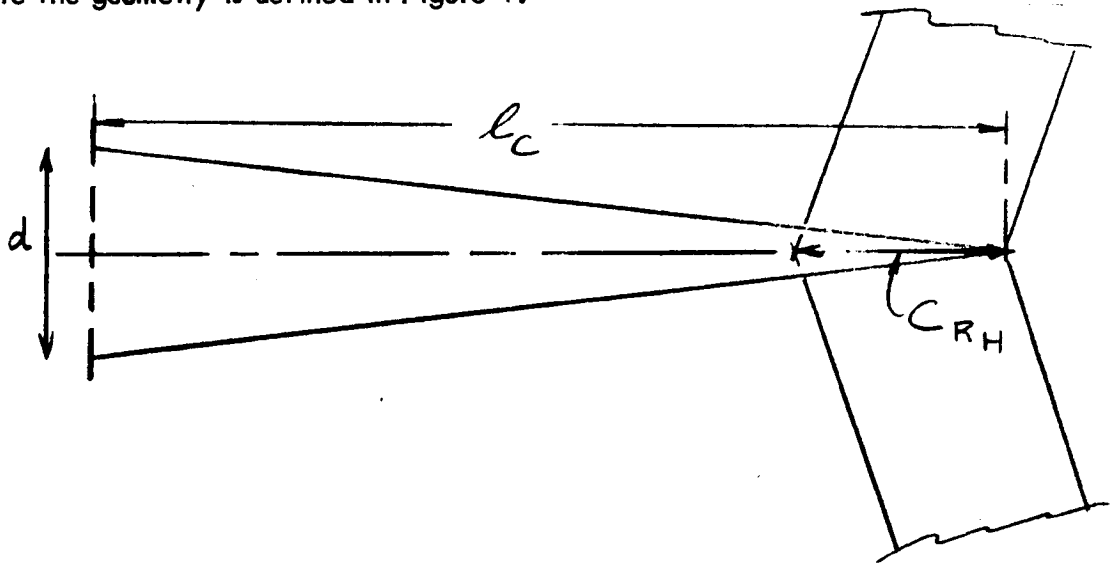

Figure 4. Horizontal Tail in Relation to Fuselage Cone

The horizontal tail drag coefficient can be written as:

$$C_{D_{o_{H.T.}}} = C_{F_H}\left[1 + L\left(\frac{t}{c}\right)_{H.T.} + 100\left(\frac{t}{c}\right)^4_{H.T.}\right] R_{L.S.} \frac{S_{WET_{H.T.}}}{S_{WING}} \quad (6)$$

where all symbols are defined in Reference 1.

The vertical tail wetted area may be approximated by:

$$S_{WET_{V.T.}} = S_V\left(2 + \underset{<<1.0}{f(t/c)}\right) - \tfrac{1}{2} C_{R_V}^2 \frac{d}{\ell_c} \quad (7)$$

where the geometry is defined in Figure 5.

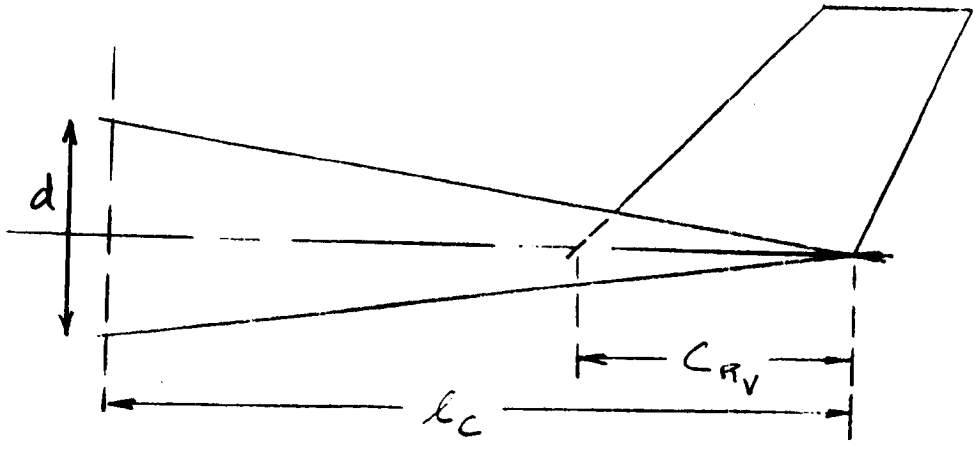

Figure 5. Vertical Tail in Relation to Fuselage Cone

The vertical tail drag coefficient can be written as:

$$C_{D_{o_{V.T.}}} = C_{f_V}\left[1 + L\left(\frac{t}{c}\right)_{V.T.} + 100\left(\frac{t}{c}\right)^4_{V.T.}\right] R_{L.S.} \frac{S_{WET_{V.T.}}}{S_{WING}} \qquad (8)$$

where all symbols are defined in Reference 1. Horizontal and vertical tail sizes are here assumed to be determined by minimum stability requirements, i.e.,:

$$C_{n_{\beta_{MIN.}}} \text{ and } C_{m_{\alpha_{MIN.}}}$$

Directional Stability - Neglecting the wing contribution, the directional stability of an airplane can be written as:

$$\begin{aligned} C_{n_\beta} &= C_{n_{\beta_B}} + C_{n_{\beta_V}} \\ &= -57.3 K_N K_{R_\ell} \frac{S_{B_s}}{S_{WING}} \frac{(\ell_N + \ell_c)}{b} + C_{L_{\alpha_V}} \frac{S_V}{S_{WING}} \frac{\ell_V}{b} \end{aligned} \qquad (9)$$

where the symbols are defined in Reference 2. The geometry is defined in Figure 6.

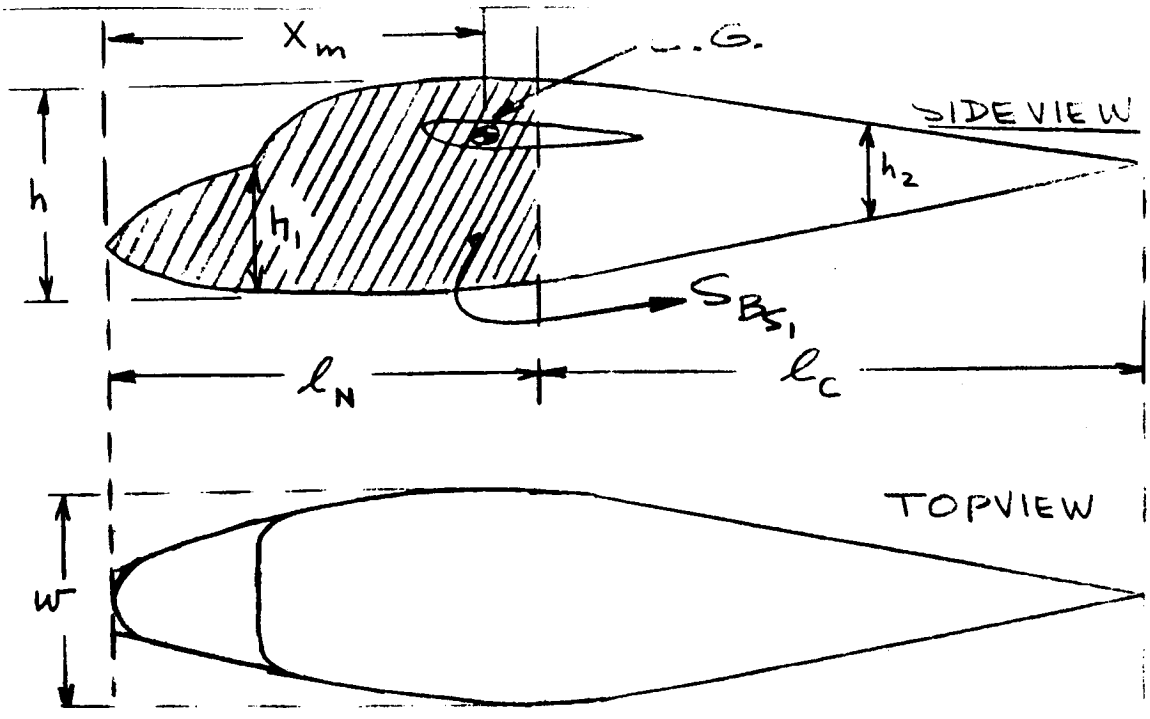

Figure 6. Fuselage Geometry for Estimating Directional Stability

Note than K_N and K_{R_ℓ} are functions of ℓ_C. Body side area, S_{B_S} can be expressed as:

$$S_{B_S} = S_{B_{S_1}} + \frac{1}{2} h \ell_C \times F \qquad (10)$$

where F is as in equation (3).

Note that:

$$C_{L_{\alpha_V}} = f(A_V, \lambda_V, \Lambda_V) \qquad (11)$$

and $\ell_V = f(\ell_C, \Lambda_{LE_V}, C_{R_V})$ as illustrated in Figure 7. (12)

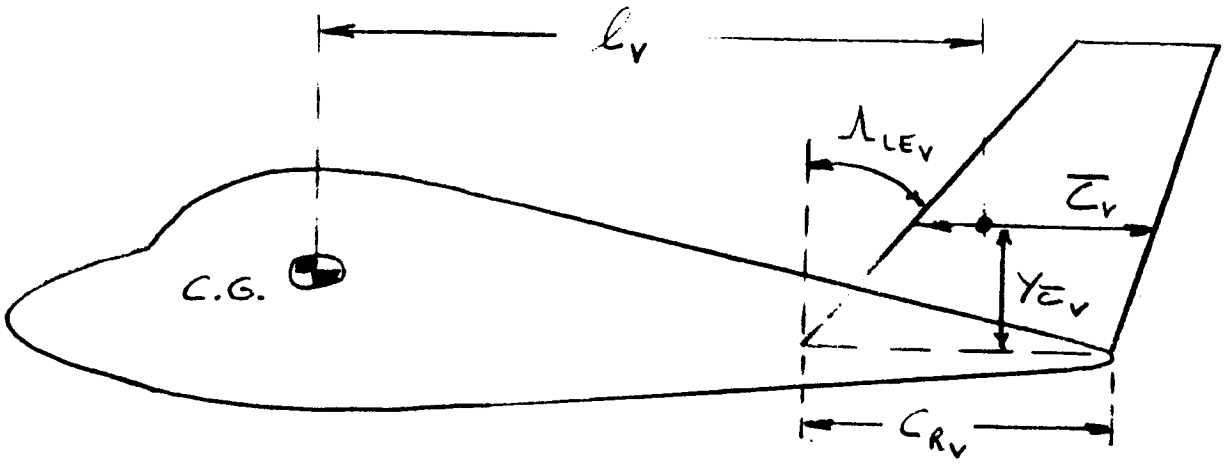

Figure 7. Definition of ℓ_v for Swept Vertical Tail

From the sketch the following equations may be deduced:

$$\ell_v = (\ell_N - x_m) + (\ell_c - c_{R_v}) + y_{\bar{c}_v} \tan \Lambda_{LE_v} + \frac{\bar{c}_v}{4} \tag{13}$$

$$y_{\bar{c}_v} = b_v \frac{1}{3}\left(\frac{1+2\lambda_v}{1+\lambda_v}\right) \tag{14}$$

$$b_v = \sqrt{S_v A_v} \tag{15}$$

$$c_{R_v} = \frac{2 S_v}{(1+\lambda_v)\sqrt{S_v A_v}} \tag{16}$$

$$\bar{c}_v = \frac{2}{3} c_{R_v}\left(\frac{1+\lambda_v+\lambda_v^2}{1+\lambda_v}\right) \tag{17}$$

Now, substitute equation (13) into (9) while using equations (14), (15), and (16):

$$C_{n_\beta} = -57.3 K_N K_{R_\ell}\left(\frac{S_{B_{S_1}} + \frac{1}{2} h \ell_c}{S_{wing}}\right)\left(\frac{\ell_N + \ell_c}{b}\right) +$$

GIVEN AS A DESIRED MINIMUM

$$+ C_{L_{\alpha_v}}{}_{RAD} \frac{S_v}{S_{wing}} \frac{1}{b}\left\{(\ell_N - x_m) + \left(\ell_c - \frac{2 S_v}{(1+\lambda_v)\sqrt{S_v A_v}}\right) + \frac{1}{3}\sqrt{S_v A_v}\left(\frac{1+2\lambda_v}{1+\lambda_v}\right)\tan \Lambda_{LE_v} + \frac{\bar{c}_v}{4}\right\} \tag{18}$$

For preselected values of $S_{B_{S_1}}$, h, S_{wing}, b, ℓ_N, A_v, λ_v and Λ_{LE_v},

it is now possible to solve for S_v for any given value of ℓ_c.

Having done that, it is possible to compute $C_{D_{o_{V.T.}}}$ as a function of l_c.

Longitudinal Stability - Longitudinal stability can be expressed by:

$$\frac{dC_m}{dC_L} = \bar{X}_{cg} - \bar{X}_{ac} \text{ , where :} \tag{19a}$$

$$\bar{X}_{ac_A} = \frac{\bar{X}_{ac_{WB}} + \frac{C_{L\alpha_H}}{C_{L\alpha_{WB}}} \frac{X_{ac_H}}{\bar{c}} \frac{S_H}{S_W}\left(1 - \frac{d\varepsilon}{d\alpha}\right)}{1 + \frac{C_{L\alpha_H}}{C_{L\alpha_W}} \frac{S_H}{S_W}\left(1 - \frac{d\varepsilon}{d\alpha}\right)} \tag{19b}$$

where all symbols are defined in Reference 3 and where:

$$X_{ac_H} = X_{ac_W} + \ell_H \tag{20}$$

as shown in Figure 8.

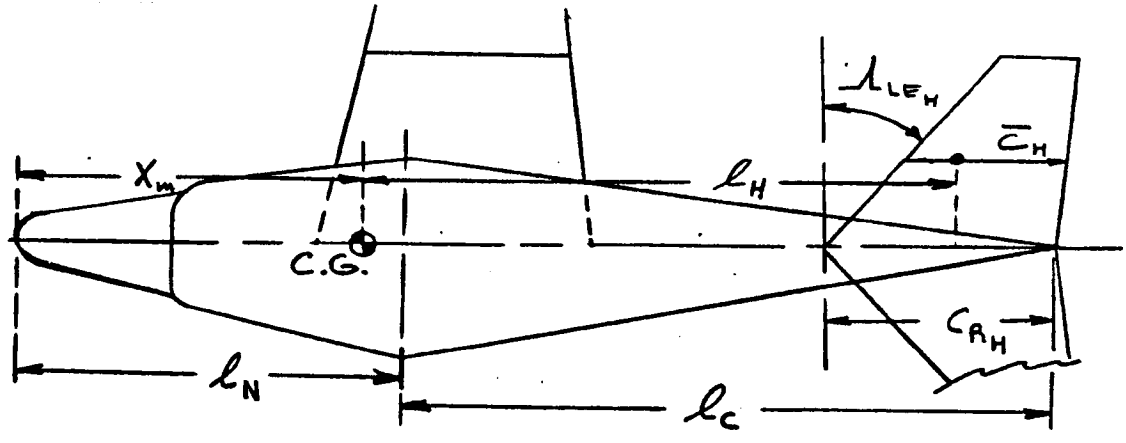

Figure 8. Definition of Horizontal Tail in Relation to Fuselage

It is assumed, that $\bar{X}_{ac_{WB}}$, $C_{L\alpha_{WB}}$, $\bar{c}$, $d\varepsilon/d\alpha$, $S_{w(ing)}$ and $\bar{X}_{ac_W}$ are known and fixed quantities.

The following expressions can be shown to hold:

$$\ell_H = (\ell_N - X_m) + (\ell_C - c_{R_H}) + \bar{y}_{c_H} \tan \Lambda_{LE_H} + \frac{\bar{c}_H}{4} \tag{21}$$

$$\bar{c}_H = \frac{2}{3} c_{R_H}\left(\frac{1 + \lambda_H + \lambda_H^2}{1 + \lambda_H}\right) \tag{22}$$

$$\bar{y}_{\bar{c}_H} = \frac{1}{2} b_H \frac{2}{3}\left(\frac{1 + 2\lambda_H}{1 + \lambda_H}\right) \tag{23}$$

$$b_H = \sqrt{S_H A_H} \tag{24}$$

$$c_{R_H} = \frac{2 S_H}{(1 + \lambda_H)\sqrt{S_H A_H}} \tag{25}$$

Plugging equation (21) into equation (20) and using equations (22) through (25) it is found that:

$$X_{ac_H} = X_{ac_W} + (\ell_N - X_m) + \left(\ell_c - \frac{2S_H}{(1+\lambda_H)\sqrt{S_H A_H}}\right) \quad (26)$$
$$+ \frac{1}{3}\sqrt{S_H A_H}\left(\frac{1+2\lambda_H}{1+\lambda_H}\right)\tan\Lambda_{LE_H} + \frac{1}{6}\left(\frac{1+\lambda_H+\lambda_H^2}{1+\lambda_H}\right)\frac{2S_H}{(1+\lambda_H)\sqrt{S_H A_H}}$$

Now, setting dC_m/dC_L = some constant value and preselecting: A_H, λ_H and Λ_{LE_H}, it is possible to solve for S_H (using equation (19) for any given value of ℓ_c. Having done this, it is possible to compute $C_{D_{oHT}}$ as a function of ℓ_c).

Parametric Study - The methods of of the previous sections allow the computation of $C_{D_{ofus}}$, $C_{D_{o_{h.t.}}}$ and $C_{D_{o_{v.t.}}}$ for given values of $\Lambda_{LE(H,V)}$ and for given values of ℓ_c.

These contributions can be plotted against ℓ_c/d as shown in Figure 9.

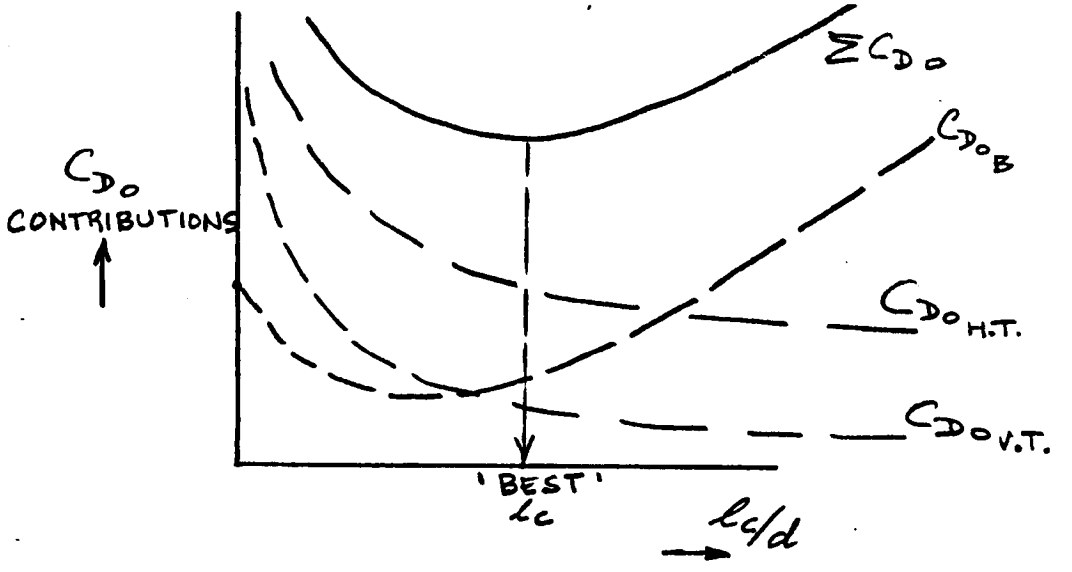

Figure 9. Plotted Results of Parametric Study

If need be this process can be repeated for a variety of empennage sweep angles. The rear fuselage length ℓ_c for minimum fuselage plus empennage drag can be readily found from Figure 9.

It would be of interest to include the effect of weight in this parametric study.

Figure 9a shows some results obtained from calculations using a Beech King Air as example. It is seen that the airplane fuselage plus empennage drag is indeed not optimum from this point of view. It would be of interest to extend this analysis to other airplanes.

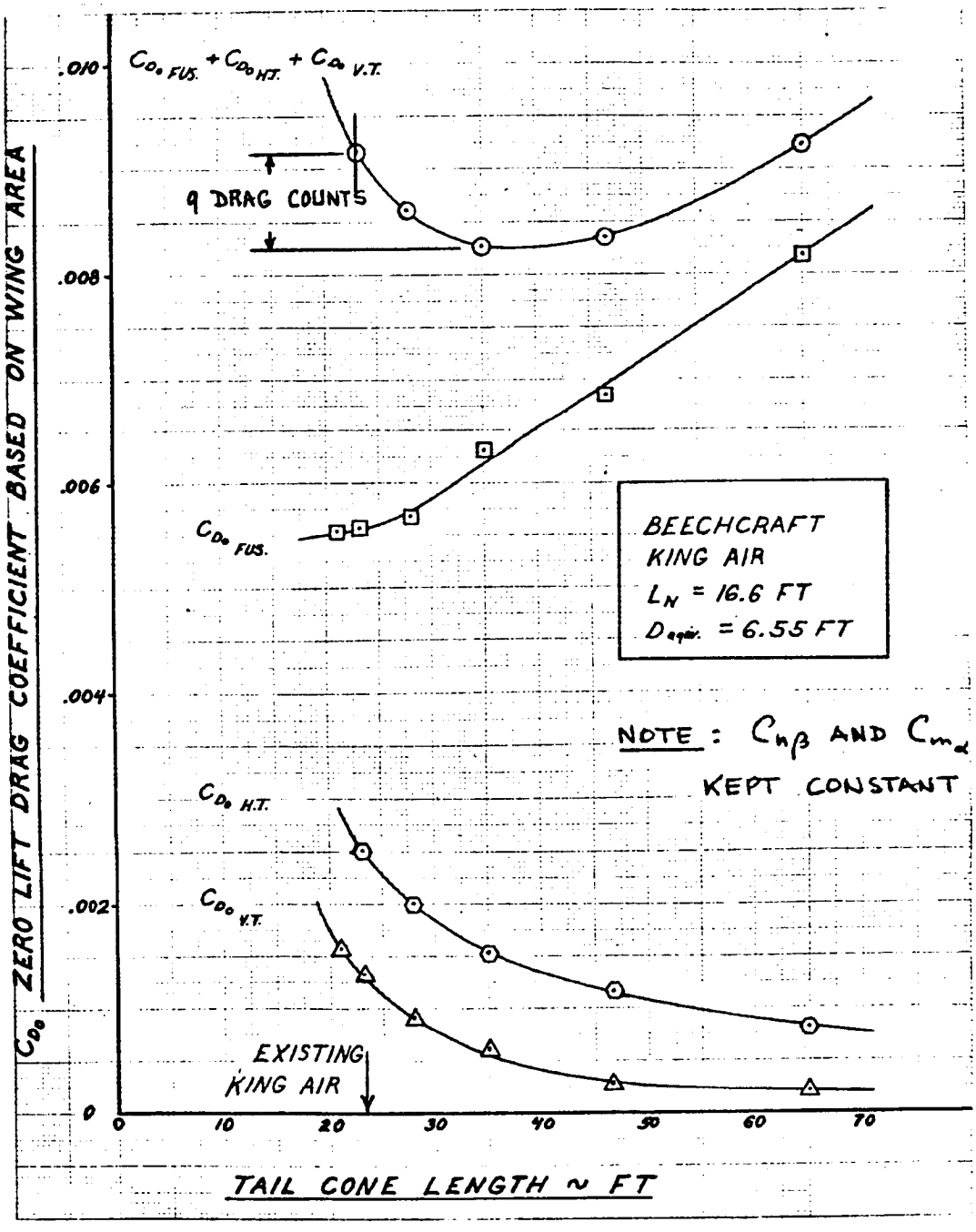

Figure 9A. Effect of Tailcone Length on Fuselage Plus Empennage Zero Lift Drag Under Constant Stability Constraints

C-2

Windshield Drag

Reference 4 presents a series of systematic data for windshield drag of small and transport type airplanes. It summarizes by stating that windshield drag can range from 20 to 1 percent of airplane drag depending on how well they are faired. This is a wide drag range!

Figures 10 and 11 illustrate the types of windshields investigated in reference 2.

Figure 12 illustrates a range of windshields found on current general aviation airplanes. It is seen that windshields of 1975 are quite different from those that prevailed in 1942. It would seem that some systematic research into this area would pay off for certain airplanes.

Surface Finish

The subject of skin waiviness and surface finish has not been brought up, because of the strong interplay with production and tooling costs. However, as shown in Figure 13 there is probably considerable room for improvement. This could be attained by a more wide spread use of metal bonding in aircraft fabrication. This way, it is feasible to maintain large areas of laminar flow over the forward part of the fuselage and capitalize on the resulting lower friction drag.

Research Needs

The fuselage typically accounts for 30 to 50 percent of total airplane drag. It seems that improvements of at least 10-20 percent could be made by taking a good research look at:

1. fuselage fineness ratio;
2. windshield drag; and
3. low cost application of metal bonding to reduce skin friction drag.

It would seem that research in the area of windshield drag should be in the form of a series of systematic wind tunnel tests.

Optimization of fuselage fineness ratio could be achieved through the development of an appropriate computer program which would also account for the effect of weight.

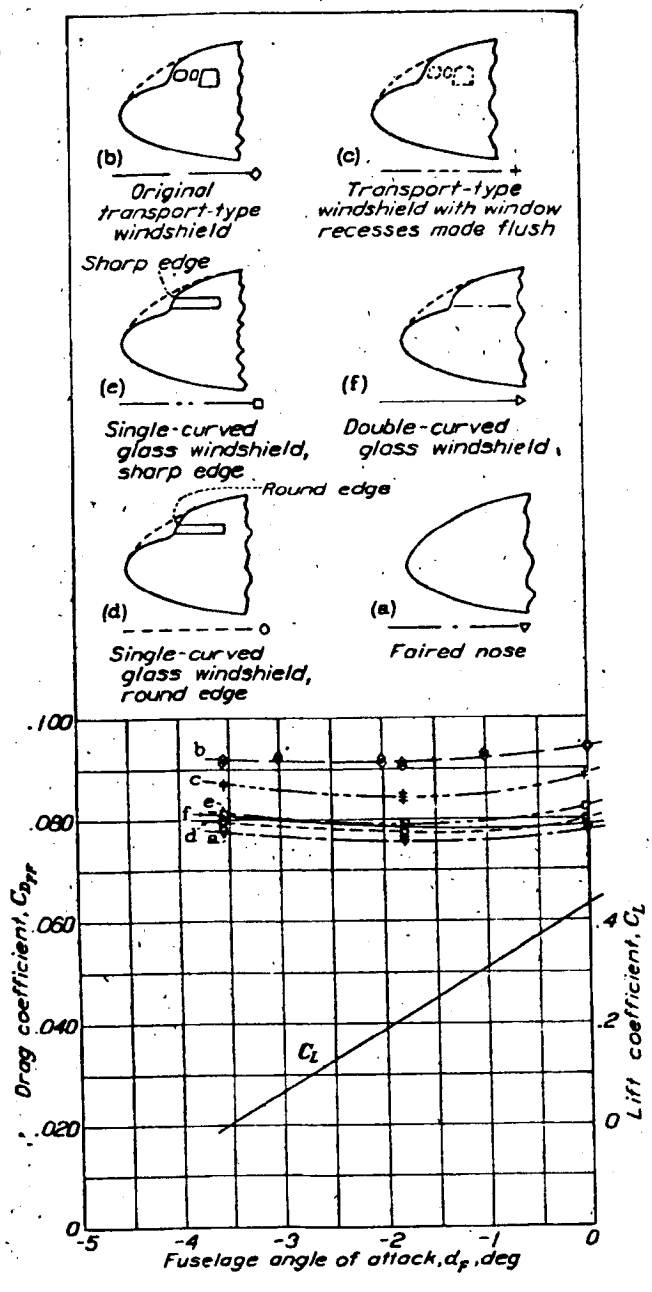

Figure 10. Drag of Fuselage with Transport-Type Windshields
M, 0.35; V, 265 mph

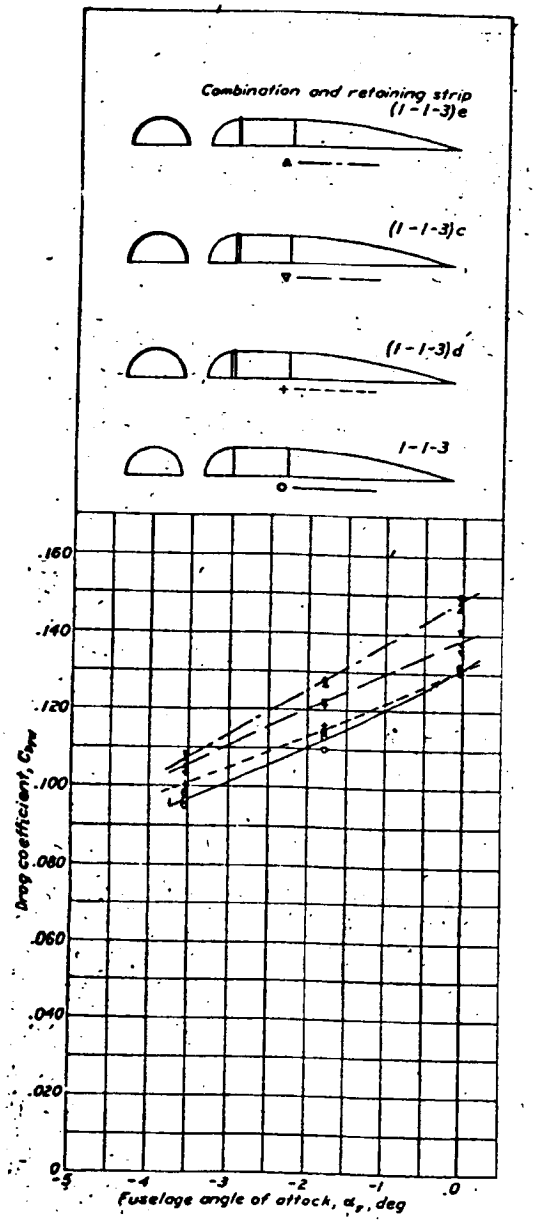

Figure 11a. Effect of Retaining Strips Combination 1-1-3, M, 0.34; V, 260 mph

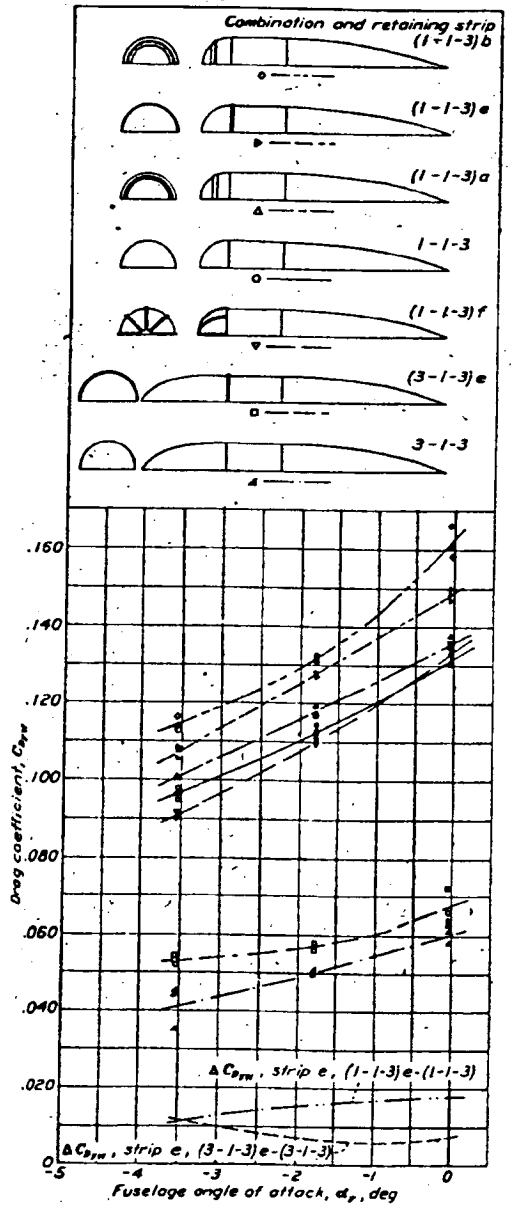

Figure 11b. Effect of Retaining Strips, Combinations 1-1-3 and 3-1-3, M, 0.34; V, 260 mph

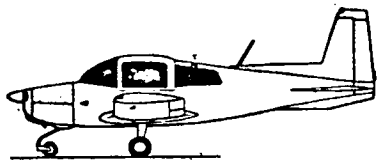

Grumman American AA-5 Traveler

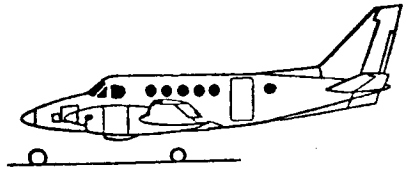

Beech King Air A100

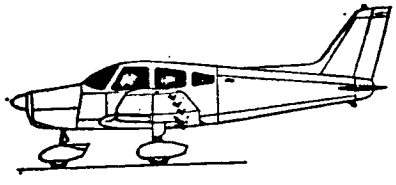

Piper Cherokee Warrior

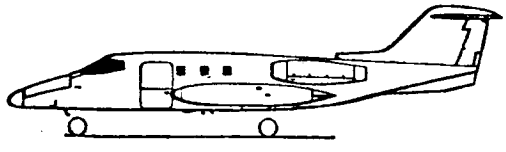

Gates Learjet 24D

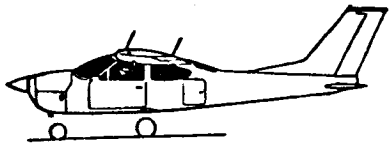

Cessna Cardinal RG

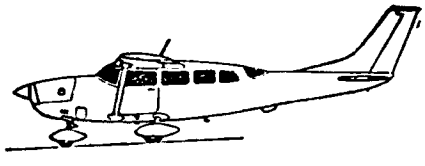

Cessna Skywagon 207

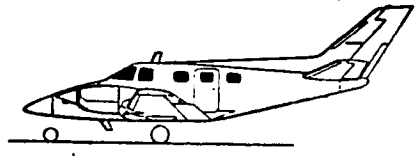

Beech Duke B60

Figure 12. Typical General Aviation Windshields for 1975

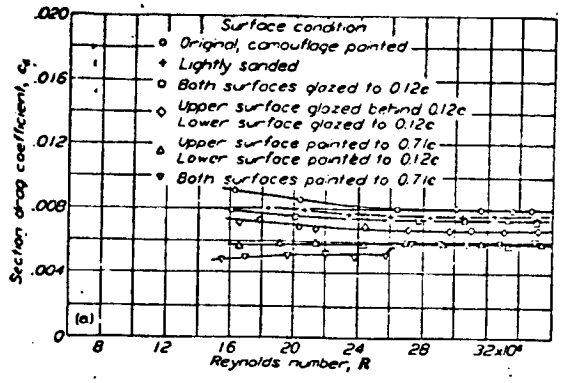

(a) Model 1, NACA 65(216)-3(16.5) (approx.) airfoil section. $c_l=0.2$.

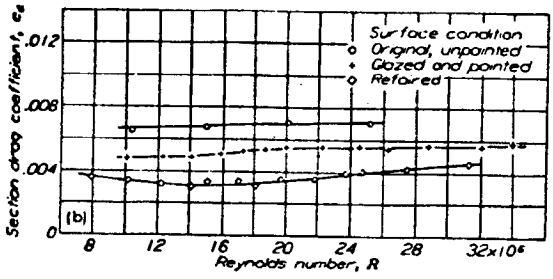

(b) Model 2, NACA 66(215)-216 (approx.) airfoil section. $c_l=0.13$.

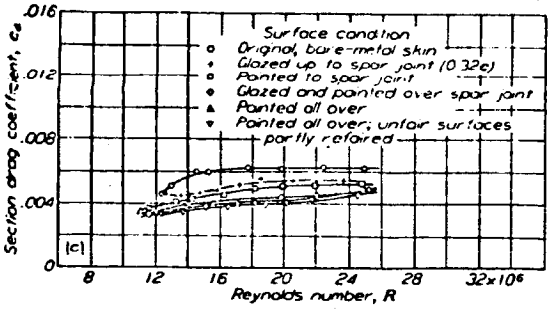

(c) Model 3, NACA 66(215)-116 airfoil section. $c_l=0.18$.

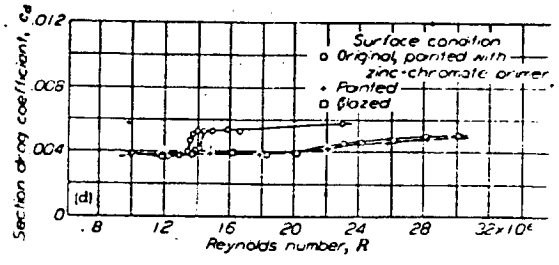

(d) Model 4, NACA 66(215)-116 $\begin{cases} a=1.0,\ c_{l_i}=0.2 \\ a=0.6,\ c_{l_i}=-0.1 \end{cases}$ airfoil section. $c_l=0.1$.

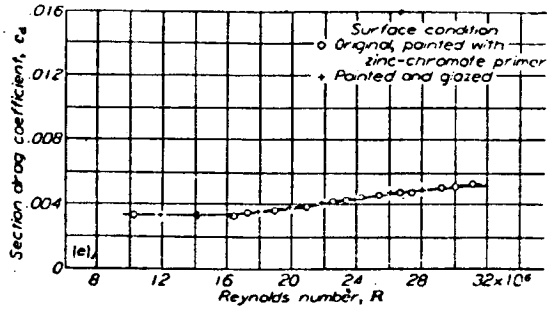

(e) Model 5, NACA 66(715)-116 $\begin{cases} a=1.0,\ c_{l_i}=0.2 \\ a=0.6,\ c_{l_i}=-0.1 \end{cases}$ airfoil section. $c_l=0.1$.

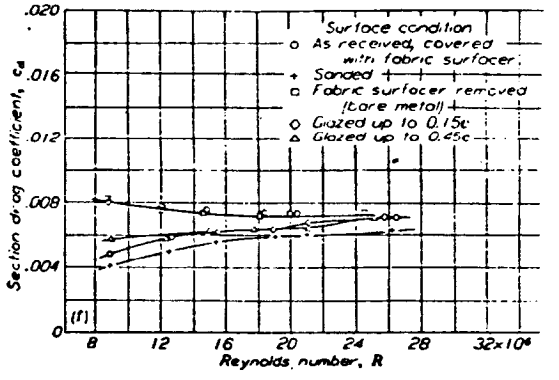

(f) Model 6, NACA 66(215)-116 practical-construction airfoil section. $c_l=0.15$ (appr

Figure 13. Effect of Surface Improvements on Drag Characteristics of Airfoil Sections

References

1. Roskam, J.; Methods for Estimating Drag Polars of Subsonic Airplanes; Published by Roskam Aviation and Engineering Corporation; 519 Boulder, Lawrence, Kansas 66044.

2. Roskam, J.; Methods for Establishing Stability and Control Derivatives of Conventional Subsonic Airplanes; Published by Roskam Aviation and Engineering Corporation; 519 Boulder, Lawrence, Kansas 66044.

3. Roskam, J.; Flight Dynamics of Rigid and Elastic Airplanes; Published by Roskam Aviation and Engineering Corporation; 519 Boulder, Lawrence, Kansas 66044.

4. Robinson, R.G. and Delano, J.B.; An Investigation of the Drag of Windshields in the 8-foot High Speed Wind Tunnel; NACA TR 730, 1942.